# Tribological properties of cobalt-based alloy coating with different cobalt contents by electro-spark deposition

**Qi-Feng Jing\*, Ye-Fa Tan**

**Abstract** The cobalt-based alloy coating with different Co contents was deposited on 45 steel by electro-spark deposition with the self-made electrode. The coating has a compact and uniform microstructure with low porosity and no visible microcracks. When Co content increases gradually, oxygen content of coating samples 1–5 decreases first and then increases in the range of 2.52 wt%–3.05 wt%; sample 3 has the lowest oxygen content of 2.52 %. Microhardness of the coating is improved remarkably compared with the substrate (HV 230.18). With Co content increasing, microhardness of the coating samples 1–5 first rises slightly and then declines rapidly in the range of HV 580.61–1052.33. Sample 3 gets the maximum of HV 1052.33, which is about 4.6 times that of the substrate. The coating presents excellent wear resistance, which first increases and then decreases when Co content increases. Sample 3 shows the best wear resistance of about 6.4 times that of the substrate. Main wear mechanism of the coating is abrasive wear and fatigue wear, along with oxidation wear under high speed or heavy load conditions.

**Keywords** Electro-spark deposition; Cobalt; Content; Microstructure; Wear resistance; Wear mechanism

Q.-F. Jing\*, Y.-F. Tan
Engineering Institute of Engineering Corps, PLA University of Science & Technology, Nanjing 210007, China
e-mail: jing_qi_feng@163.com

Q.-F. Jing
Unit 78649 of PLA, Chengdu 610200, China

## 1 Introduction

A cobalt-based alloy is a hard alloy that can resist many kinds of wear, corrosion, and high temperature oxidation. It also has other properties of high hardness, high intensity, good thermal stability and resistance to hot corrosion and thermal fatigue, and so on [1, 2]. Co is a silvery-white, hard transition metal with high strength and good creep resistance; proper proportion of Co in a hard alloy (such as W-$x$Co, Stellite alloy, etc.) can improve their intensity, wear resistance, and corrosion resistance significantly [3–5]. With good wear resistance and low surface roughness, the cobalt-based alloy is used to make seal valve. By good thermal stability and resistance to high temperature, it is also used to produce the blade of an aviation engine and gas turbine and the nozzle of a diesel engine. Nowadays, the cobalt-based alloy has been widely used in aviation, aerospace, military, medical treatment, etc. Moreover, it is also suitable for surface strengthening and fracture repair of metal parts.

Electro-spark deposition (ESD) is a pulsed arc microwelding technique for surface strengthening, which is also called electro-spark alloying (ESA). During the deposition process, high frequency pulse discharge of the ESD system produces instantaneous high temperature between the electrode and the substrate, and thus the consumable electrode material is melted and deposited onto the substrate surface to form a strengthening coating with special tribological properties and mechanical properties. ESD technology has many obvious advantages in comparison with other deposition methods, such as simplicity and portability of equipment, low cost, low heat input, high cooling rate, metallurgical bonding with the substrate, no thermal distortion of the substrate, cleanliness and safety, etc. It has been widely applied to surface repair, surface strengthening, fracture welding, and other fields [6–13].

In this work, a cobalt-based alloy powder of C, Cr, Si, W, Fe, Mo, Ni, Mn, and different contents of Co was prepared based on numerous previous experimentations, and then the prepared cobalt-based alloy powder was used to make a strengthening electrode for ESD. After that, the coating was deposited on 45 steel by ESD technology with the self-made electrode. A series of experimentations were conducted to research the influence of Co content on microstructure, microhardness, and tribological properties of the coating.

## 2 Experimental

### 2.1 Electrode preparation

The cobalt-based alloy powder was prepared with a chemical composition of 5.8 % C, 51 % Cr, 2.6 % Si, 21 % W, 8 % Fe, 2.4 % Mo, 6.4 % Ni, 2.8 % Mn, and different contents of Co % (mass fraction). With sodium silicate as the agglomerate, the cobalt-based alloy powder was used to make an electrode via pressing (in a copper model at a pressure of 6 MPa), air drying, and thermal sintering (at 1,400 °C lasting for 12 h). The self-made electrode was 4 mm in diameter and 30 mm in length. Co content in the electrode is given in Table 1; with progressive increase in sample number, Co content in the electrode or coating sample increases.

### 2.2 Coating preparation

45 steel (3 mm in thickness) was selected as the substrate, and the self-made electrode with different Co contents was used for ESD. The coating was deposited on 45 steel by a DZ2000 ESD system in an argon atmosphere. Deposition parameters were voltage of 110 V, power of 1,600 W, capacitance of 360 μF, gas flow of 6 L·min$^{-1}$, and deposition rate of 4 min·cm$^{-2}$. By grinding and polishing, the coating was 0.3 mm in thickness and 0.5 μm in roughness. By means of wire cutting, cleaning, and etching with 4 % HNO$_3$ ethanol solution, the coating was made into 10 mm × 10 mm × 3.3 mm samples. The number of the coating samples is presented in Table 1, with the same sample number, the coating, and the electrode has the same Co content.

### 2.3 Tribological tests and surface analysis

Tribological tests were conducted on a TH500 ball-disk abrasion tester. Test conditions were carried out as follows:

**Table 1** Co content in electrodes/samples (wt%)

| Electrode/sample nos. | 1 | 2 | 3 | 4 | 5 |
|---|---|---|---|---|---|
| Co content | 34.3 | 41.5 | 45.8 | 50.6 | 55.1 |

temperature of 25 °C, relative humidity of 60 % RH (relative humidity), and test time of 30 min. GCr15 steel ball was used as friction pair in a diameter of 5 mm, a roughness of 0.06 μm, and a microhardness of HRC 66. Mass loss was measured by a TG328B analytical balance (accuracy of 0.1 mg).

Microhardness of the coating was measured by an FM-7 microhardness tester at a set load of 4.9 N and a dwell time of 15 s. Microstructure and morphology of the coating were researched by a DMM-330C optical microscope (OM) and a XQUANTA200 scanning electron microscope (SEM). Chemical composition of the coating and the worn surface was analyzed by an energy dispersive spectroscope (EDS) GENSIS2000 model.

## 3 Results and discussion

### 3.1 Microstructure of the coating

Surface morphology and oxygen content of the coating are given in Fig. 1. Macromorphology of the coating looks like an orange peel (Fig. 1a). That is because during ESD process, electro-spark discharge produces a high temperature of 8,000–25,000 °C to form a discharge micro-zone between the electrode and the substrate; the electrode material is melted and then sputters from the electrode top to the substrate surface. When the electrode material cools and solidifies, it produces a strengthening point and a discharge pit; the discharge pit diffuses around from the pit center (Fig. 1b). After repeated deposition, numerous strengthening points and discharge pits fuse and overlap with each other to form the strengthening coating. Therefore, the coating has compact and uniform microstructure with low porosity and no visible microcracks [14].

The EDS analysis of the coating samples shows that oxygen element exists in the coating; with Co content increasing gradually, oxygen content of samples 1–5 decreases first and then increases in the range of 2.52 wt%–3.05 wt%; sample 3 has the lowest oxygen content of 2.52 % (Fig. 1c) because, during the ESD process, shielding gas around the electrode is partly broken down by the high temperature of pulse discharge, then the electrode material reacts with the surrounding air to form the oxide that exists in the coating [15]. As a result of good high temperature resistance of cobalt-based alloy, oxide content in the coating declines when Co content first increases. However, when Co content in the electrode exceeds the especial proportion, oxygen content in the coating goes up when Co content further increases because Co will be oxidized when temperature is higher than 300 °C. During the deposition process, additional Co transits to the substrate in ionic form, except reacts with W and C (to form
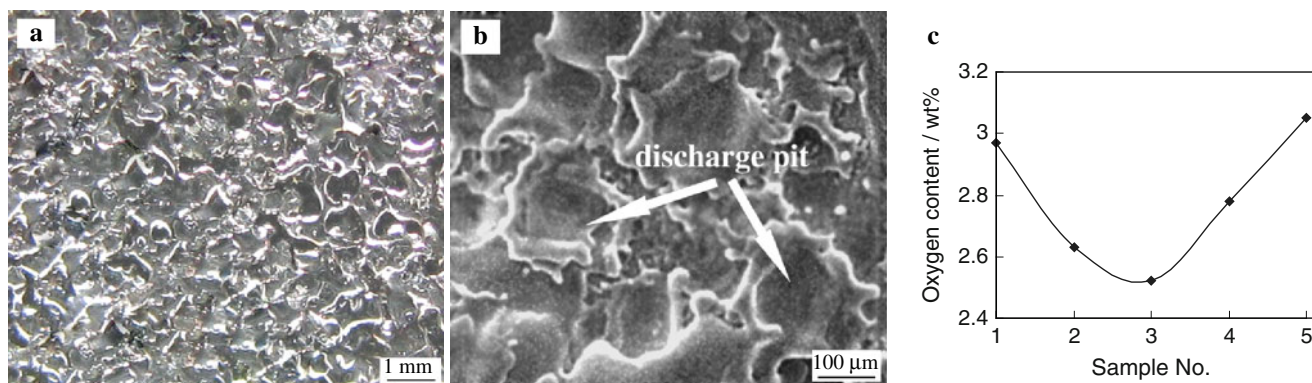
**Fig. 1** Surface morphology (SEM images) and oxygen content of coating: **a** macromorphology of coating sample 3, **b** discharge pit of coating sample 3, **c** oxygen content of coating samples 1–5 by EDS analysis

strengthening phase of $CoC_x$, $Co_6W_6C$, WC), then cobalt ion is oxidized to generate oxide.

Morphology and element distribution of a cross section of the coating are presented in Fig. 2. As shown in Fig. 2a, the white-bright layer in the middle of this figure is the bonding zone, the upper side of the figure is the strengthening coating, and the underside is the substrate. The coating has a compact and uniform microstructure, and the grain size of the coating is smaller than that of the substrate. One reason for the smaller grain size of the coating is that the discharge time of the capacitor for ESD is very short ($1 \times 10^{-6}$–$1 \times 10^{-5}$ s), whereas cooling rate of the coating is very high ($1 \times 10^5$–$1 \times 10^6$ °C·s$^{-1}$), which can prevent grain growth of the coating. Another reason is that the strengthening phase is remelted and recrystallized by the effect of repeated pulse discharge during the ESD process, which refines the microstructure effectively. Furthermore, the change of stress field and equivalent strain of temperature in the coating surface is also responsible for microstructure refinement. Further observation shows that the coating-substrate boundary has no obvious microcracks and micropores. It makes evidence of high adhesion between the coating and the substrate.

Along the white line in Fig. 2a, EDS line scanning was conducted to analyze element distribution in the cross section of the coating. Figure 2b shows that the content of the electrode material (Co, Cr, W, etc.) is stable in the coating, but declines sharply in the bonding zone. Differently, the substrate material, such as Fe, increases rapidly in the bonding zone toward the substrate direction. It indicates that the materials of the electrode and the substrate diffuse and infiltrate with each other in the bonding zone. This occurs mainly because, at the initial stage of the ESD process, under the effect of high temperature, when the electrode material (Co, Cr, W, etc.) transits to the substrate, the substrate material (Fe) transfers to the electrode. It can also be seen in Fig. 2a that the electrode material diffuses below the substrate surface, and there is
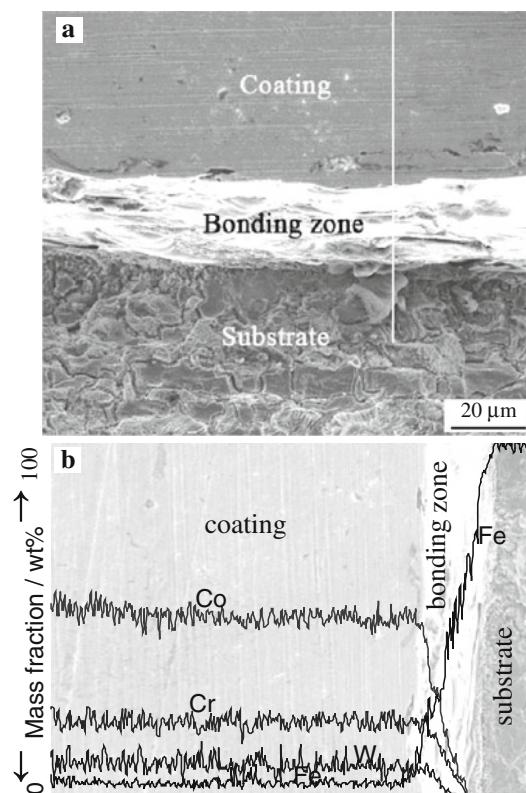


**Fig. 2** Cross-section morphology (SEM images) (**a**) and element distribution of cross section (**b**) of coating sample 3

no obvious interface between the coating and the substrate. The results indicate that the coating creates metallurgical bonding with the substrate [16].

## 3.2 Effect of Co content on microhardness of the coating

Microhardness of different coating samples is shown in Fig. 3. Figure 3a shows that the microhardness of the coating is improved remarkably compared with the

substrate (HV 230.18). When Co content increases, the microhardness of coating samples 1–5 first rises slightly and then declines rapidly in the range of HV 580.61–1052.33. Sample 3 gets the maximum of HV 1052.33, which is about 4.6 times that of the substrate because, as mentioned before, Co is a silvery-white, hard transition metal with high strength and good creep resistance; it improves intensity and wear resistance of metal parts significantly, so microhardness of the coating increases when Co content first increases. Furthermore, the strengthening phase, such as $CoC_x$, $Co_6W_6C$, WC (formed by Co, W, and C during ESD process), has much higher hardness than the substrate, which improves microhardness of the coating remarkably. In addition, as analyzed before, cobalt ion in the coating is distributed in the grain boundary, which refines microstructure of the coating effectively; it is also responsible for hardness enhancement of the coating. Therefore, when Co content first increases, microhardness of the coating increases. However, when Co content exceeds the special proportion, microhardness of the coating decreases rapidly because, on the one hand, Co has better tractility than Fe, and additional Co in the coating makes the coating become soft to some extent. On the other hand, the higher the Co content, the lower the strengthening phase content of the coating, which results in microhardness reduction of the coating. Third, oxide formed by an additional Co element makes the coating appear as microcracks and micropores, which also helps in microhardness reduction of the coating.

Microhardness of a cross section of coating sample 3 along the depth direction is shown in Fig. 3b. The coating has high and stable microhardness with an average value of HV 1027.64 and a maximum value of HV 1052.33, which locates at 0.1 mm below the coating surface because such defects as discharge pits and micropores in the coating surface make the surface hardness slightly lower than that in the internal coating. Further observation shows that microhardness decreases in the bonding zone. As mentioned before, the electrode material in the bonding zone is infiltrated and diluted by the substrate material; thus, microhardness in the bonding zone declines.

### 3.3 Effect of Co content on tribological properties of the coating

#### 3.3.1 Effect of Co content on tribological properties of the coating under different load conditions

Tribological tests at different loads were conducted under the following conditions: frequency was set at 8 Hz (equal to friction speed of 0.08 m·s$^{-1}$), and test loads were 4, 6, 8, and 10 N. Mass loss and friction coefficient of coating samples 1–5 versus load are presented in Fig. 4. As seen in
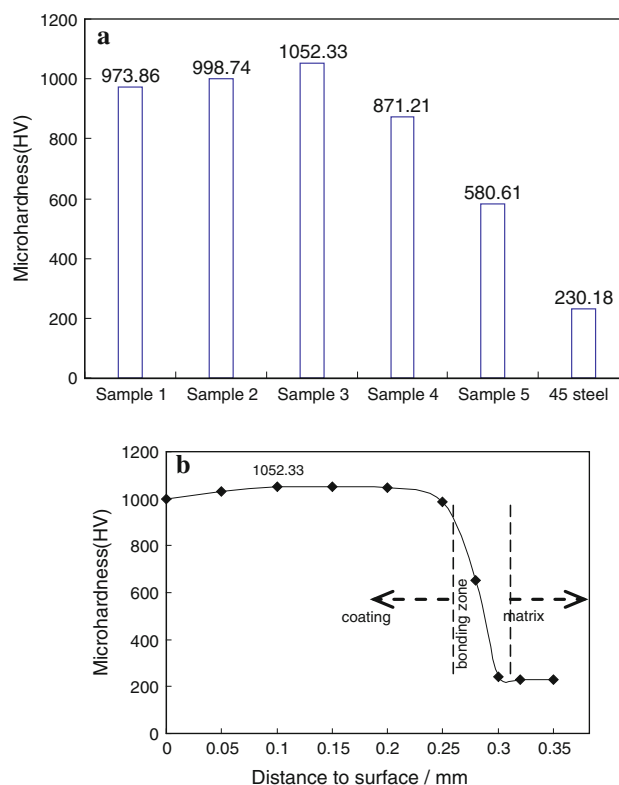


**Fig. 3** Microhardness of coating samples (**a**) and microhardness of cross section of coating sample 3 along depth direction (**b**)

Fig. 4a, when load increases, the mass loss of each coating sample increases. Mass loss of the coating increases slowly at 4–8 N, but increases rapidly at 8–10 N. Mass loss of the substrate (1.2–6.9 mg) is much higher than that of the coating. Figure 4a also shows that, with Co content gradually increasing, mass loss of coating samples 1–5 decreases first and then increases, and sample 3 shows the best wear resistance.

When load increases, the friction coefficient of each coating sample first decreases and then increases. When Co content increases, friction coefficient of coating samples 1–5 first declines and then rises, and sample 3 has the minimum value (Fig. 4b). Friction coefficient of samples 1–3 decreases at 4–8 N and increases at 8–10 N. Differently, the friction coefficient of samples 4–5 has no obvious fluctuation at 4–8 N and increases rapidly at 8–10 N. The results indicate that Co content has an obvious effect on tribological properties of the coating under different load conditions.

#### 3.3.2 Effect of Co content on tribological properties of the coating under different speed conditions

Tribological tests at different speeds were conducted under the following conditions: load was 8 N, and frequencies were 4, 6, 8, 10 Hz (equal to speed of 0.04, 0.06, 0.08,
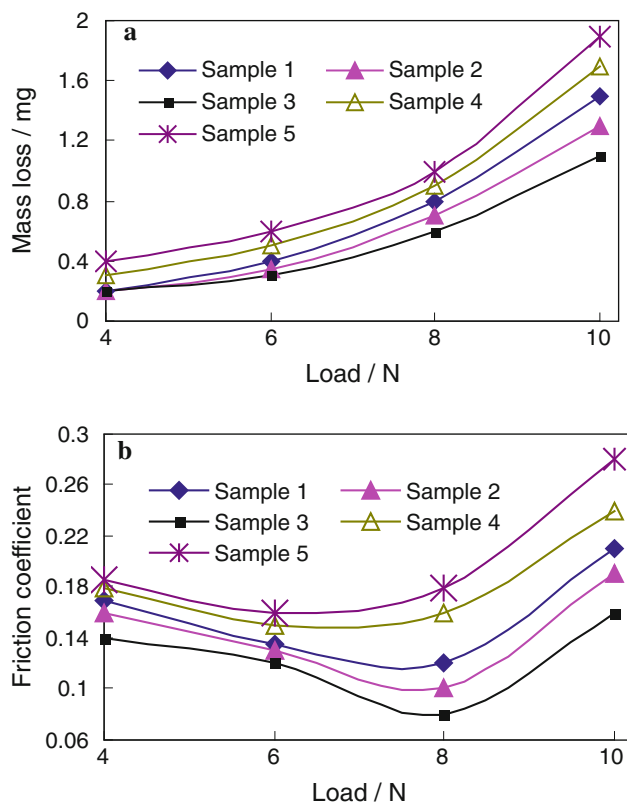
Fig. 4 Mass loss (**a**) and friction coefficient (**b**) of coating samples 1–5 versus load at 0.08 m·s$^{-1}$



Fig. 5 Mass loss (**a**) and friction coefficient (**b**) of coating samples 1–5 versus speed at 8 N

0.1 m·s$^{-1}$, respectively). Figure 5 presents mass loss and friction coefficient of coating samples 1–5 versus speed. As seen in Fig. 5a, with speed increasing, the mass loss of each coating sample increases, but mass loss of the substrate (1.3–7.6 mg) is much higher than that of the coating. When Co content increases, mass loss of coating samples 1–5 diminishes first and then goes up. Sample 3 has the best wear resistance, which is about 6.4 times that of the substrate.

Figure 5b shows that, when speed increases, friction coefficient of each coating sample first declines and then ascends. When Co content increases, friction coefficient of coating samples 1–5 decreases first and then increases. Sample 3 gets the minimal friction coefficient, which decreases at 0.04–0.08 m·s$^{-1}$ and increases at 0.08–0.1 m·s$^{-1}$. However, the friction coefficient of samples 1, 2, 4, and 5 decreases at 0.04–0.06 m·s$^{-1}$ and increases at 0.06–0.1 m·s$^{-1}$. It indicates that the proper proportion of Co content can reduce friction coefficient effectively.

### 3.3.3 Wear mechanism of the cobalt-based coating

The coating with high strength and hardness has good peeling resistance and adhesion resistance, and accordingly the coatin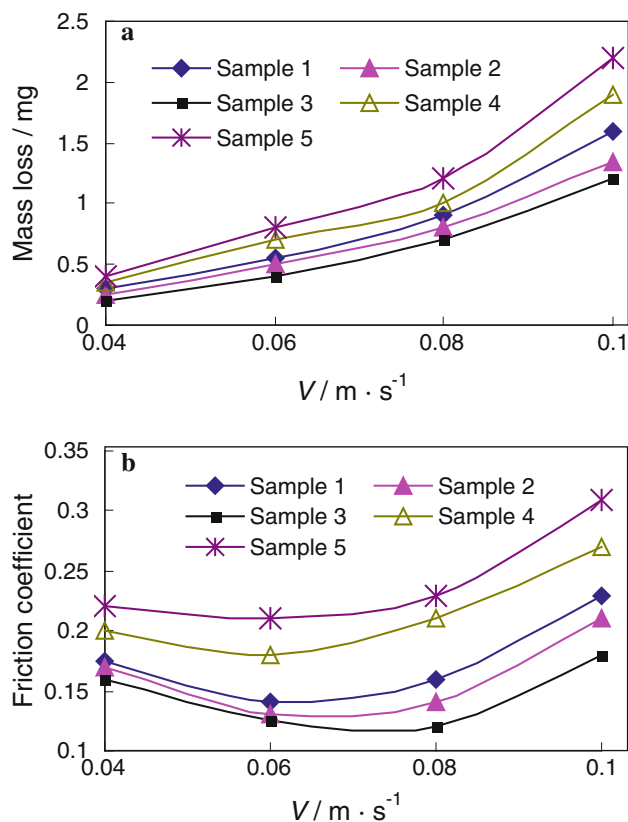g surface is worn slightly with some capillary furrows out of an obvious peeling phenomenon at low load or low speed stage (Fig. 6a, b); the main wear mechanism of the coating is abrasive wear. With load or speed increasing, the coating material becomes soft, which is affected by accumulated temperature, and thus the worn surface of the coating appears like obvious furrows by micro-cutting, and peeling particles filling in the furrows play a lubrication role; therefore, friction coefficient of the coating decreases.

When load or speed further increases to heavy load or high speed conditions, the temperature of the worn surface further rises under the effect of accumulated heat, and the coating material becomes harder. Under the repeated action of normal stress and local high temperature, the coating surface appears to have plastic deformation and fatigue damage, such as a serious scratch and peeling phenomenon (Fig. 6c, d). Then, fatigue damage accumulates to form fatigue cracks in the worn surface, and accordingly friction coefficient of the worn surface increases and coating wear aggravates. The main mechanism of the coating under heavy load or high speed conditions is fatigue wear.

Oxygen content in the worn surface of coating samples 1–5 by EDS analysis under heavy load or high speed is
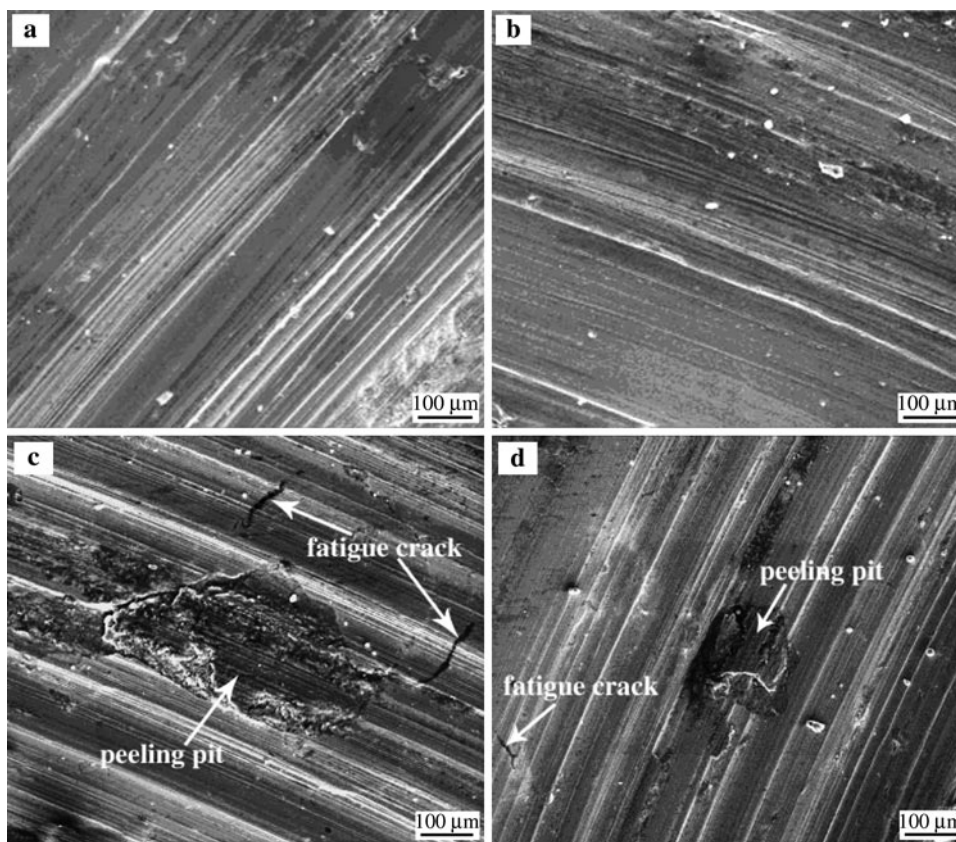
**Fig. 6** Worn morphology (SEM images) of sample 3 at different load and speed condition: **a** 4 N, 0.08 m·s$^{-1}$; **b** 0.04 m·s$^{-1}$, 8 N; **c** 10 N, 0.08 m·s$^{-1}$; **d** 0.1 m·s$^{-1}$, 8 N

presented in Fig. 7. The figure shows that, under heavy load or high speed conditions, oxygen content in the worn surface of coating samples 1–5 is much higher than that of the original coating; this decreases first and then increases with Co content increasing because local high temperature produced by heavy load or high speed makes the worn surface form a high temperature micro-zone. Strengthening material in this micro-zone comes into contact with air and appears to show oxidization phenomenon. The results indicate that the coating has oxidation wear under heavy load or high speed conditions.

## 4 Conclusion

The cobalt-based alloy coating with different Co contents was deposited on 45 steel by ESD with the self-made electrode. The coating has a compact and uniform microstructure with low porosity and no visible microcracks. With Co content increasing gradually, the oxygen content of coating samples 1–5 decreases first and then increases in the range of 2.52 wt%–3.05 wt%; sample 3 has the lowest oxygen content of 2.52 %. Microhardness of the coating is improved remarkably compared with the substrate (HV
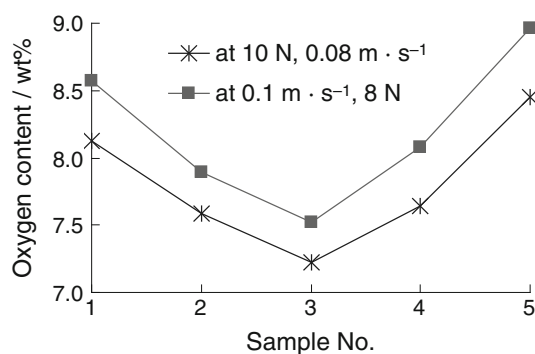


**Fig. 7** Oxygen content in worn surface of coating samples 1–5 by EDS analysis at heavy load condition (10 N, 0.08 m·s$^{-1}$) and high speed condition (0.1 m·s$^{-1}$, 8 N)

230.18). With Co content increasing, microhardness of the coating samples first rises slightly and then declines rapidly in the range of HV 580.61–1052.33. Sample 3 gets the maximum of HV 1052.33, which is about 4.6 times that of the substrate. The coating presents excellent wear resistance. With Co content increasing, wear resistance of the coating samples first increases and then decreases. Sample 3 shows the best wear resistance of about 6.4 times that of the substrate. The main wear mechanism of the coating is

abrasive wear and fatigue wear, along with oxidation wear under high speed or heavy load conditions.

## References

[1] Birol Y. Inconel 617 and Stellite 6 alloys for tooling in thixo-forming of steels. Trans Nonferrous Met Soc China. 2010; 20(9):1656.

[2] Jin G, Xu BS, Wang HD, Li QF, Wei SC. Microstructure and wear resistance of electro-thermal explosion sprayed Stellite coating used for remanufacturing. J Cent South Univ Technol. 2005;12(S2):207.

[3] Wang JS, Meng HM, Yu HY, Fan ZS, Sun DB. Wear characteristics of spheroidal graphite roll WC-8Co coating produced by electro-spark deposition. Rare Met. 2010;29(2):174.

[4] Pan L, Gao WZ, Tao XQ, Xia CH. Evaluation on microtructures and properties of laser cladding layer for WFLC-11 Co-based alloy. Rare Met Mater Eng. 2007;36(8):1444.

[5] Pang CS, Luo J, Guo ZM. Microstructure and properties of ultrafine WC-10Co composites with chemically doped VC. Rare Met. 2011;30(2):183.

[6] Wang MC, Wang WF, Xie YJ, Zhang J. Electro-spark epitaxial deposition of NiCoCrAlYTa alloy on directionally solidified nickel-based superallo. Trans Nonferrous Met Soc China. 2010; 20(5):795.

[7] Dolinšek S, Tušek J, Kampuš Z. Electrospark deposition (ESD) for surfacing of direct metal laser sintering (DMLS) tools. In:

[8] Radek N. Experimental investigations of the Cu-Mo and Cu-Ti electro-spark coatings modified by laser beam. Adv Manuf Sci Technol. 2008;32(2):53.

[9] Brochu M, Portillo JG, Milligan J, Heard DW. Development of metastable solidification structures using the electrospark deposition process. Open Surf Sci J. 2011;3:105.

[10] Verbitchi V, Ciuca C, Cojocaru R. Electro-spark coating with special materials. Nonconv Technol Rev. 2011;15(1):57.

[11] Sartwell BD, Legg KO, Price N, Aylor D, Champagne V, Pepi M, Pollard T. Electrospark deposition for depot-and field-level component repair and replacement of hard chromium plating: department of defense. Environmental Security Technology Certification Program (ESTCP). Washington, DC; 2006.

[12] Chen Z, Zhou Y. Surface modification of resistance welding electrode by electro-spark deposited composite coatings: part I. Coat charact Surf Coat Technol. 2006;201(3–4):1503.

[13] Evgeny AL. Development of electro-spark alloying (ESA) and thermo-reactive electro-spark surface strengthening (TRESS) technologies and set of equipment with attachments for mechanization. Moscow State Institute of Steel and Alloys (Technological University). Moscow; 2006.

[14] Tušek J, Kosecl L, Lešnjak A, Muhič T. Electrospark deposition for die repair. Metalurgija. 2012;51(1):17.

[15] Li ZW, Gao W, He YD. Protection of a Ti3Al-Nb alloy by electro-spark deposition coating. Scripta Materialia. 2001;45(9): 1099.

[16] Tang SK, Nguyen TC, Zhou Y. Materials transfer in electro-spark deposition of TiCp/Ni metal-matrix composite coating on Cu substrate. Weld J. 2010;89(8):172.

7th International scientific conference on achievements in mechanical & materials engineering, Gliwice, 2003: 1103.